Dynamic Beam Switching of Vertical-Cavity Surface-Emitting Lasers with Integrated Optical Beam Routers

L. Fan, M. C. Wu, *Member, IEEE,* H. C. Lee, and P. Grodzinski

***Abstract*—Dynamic beam switching of vertical-cavity surface-emitting lasers (VCSEL's) have been demonstrated for the first time using integrated optical beam routers. The output beam of the VCSEL is switched electrically between two different emission angles. High-speed switching up to 2 GHz has been achieved with an 8 μm × 8 μm device. Such beam-steering devices are particularly suitable for optical interconnect and photonic switching applications. By integrating the beam routers with VCSEL's, the complexity and size of the switching nodes are significantly reduced.**

***Index Terms*—Beam steering, laser beam steering, multistage interconnection network, optical interconnections, optical phase shifters, optical switches, space division switching, surface-emitting lasers.**

I. Introduction

OPTICAL interconnect can significantly improve the performance of massively parallel computers with a large number of processors, whose performance is limited by the communications among processors [1]. It has high parallelism, high spatial and temporal bandwidth, and is free from electromagnetic interference [2]. More importantly, many sophisticated interconnection networks such as hypercube and multistage networks can be readily implemented in the optical domain [3]. Early attempts to incorporate optical interconnect in massively parallel processors use high-speed optical fiber links to replace electric wires. Recently, there is a growing interest to use free space optical interconnections to further exploit the parallelism of photons for dense, reconfigurable interconnections [4].

Vertical-cavity surface-emitting lasers (VCSEL's) offer many advantages for optical interconnections, including low threshold currents, small beam divergence angles, wafer scale processing and testing, and the ability to form two-dimensional arrays [5]. Recently, VCSEL's with threshold current lower than 100 μA [6], and power conversion efficiency of 50% [7] have been demonstrated, making them ideal candidates for low-power interconnection networks. Even though the active optoelectronic devices can be very densely packed in monolithic two-dimensional arrays, the volume of optical interconnection network is usually dominated by passive optical elements such as lenses, gratings, or holograms [8]. By integrating the optical beam routing elements with the active optoelectronic devices, substantial reduction in the volume of the interconnection network can be achieved. Attempts have been made to integrate optical beam routers with edge-emitting lasers [9], [10]. However, such structure is limited to one-dimensional steering. Previously, we have proposed a novel VCSEL with monolithically integrated optical beam router. Optical beams emitted from the VCSEL have been steered away from the surface-normal direction by as large as 9.6° [11].

In this letter, we report on the dynamic beam switching properties of the VCSEL with monolithic optical beam router. The emitting angles are switched electrically between 0° and 2.9°. Dynamic switching up to 2 GHz has been demonstrated. The active area of the beam-steering VCSEL (8 μm × 8 μm) is comparable to that of standard VCSEL, therefore, most advantages of the VCSEL's such as low threshold current and high beam quality are maintained. By integrating such beam-switching VCSEL's with different switching angles into two-dimensional arrays, various types of optical interconnection networks, such as banyan network, can be constructed on a monolithic substrate.

II. Design

The schematic structure of the VCSEL with integrated beam router is shown in Fig. 1(a). A phase shifter is created on half of the VCSEL surface by etching the cap layer of the VCSEL by half wavelength. Alternatively, it can also be realized by depositing dielectric materials on the VCSEL surface). If the VCSEL operates in fundamental transverse mode, the output beam has a uniform phase front before passing the phase shifter. Half of the wavefront of the emitting light will experience an extra phase delay after passing through the phase shifter. The output beam is steered away from the original surface-normal direction as a result of the interference between the phase-shifted and nonphase-shifted beams.

It is known that the reflectivity of the distributed Bragg reflector (DBR) mirror is very sensitive to the terminating phase of the DBR. As pointed out in [11], the reflectivity of the DBR is not changed by the phase-shifter if its thickness

Manuscript received October 28, 1996; revised January 3, 1997. The work of L. Fan, M. C. Wu at UCLA was supported by DARPA via Army Research Laboratory under Contract DAAL01-93-K-3353 and by the Packard Foundation.

L. Fan and M. C. Wu are with University of California, Los Angeles, Electrical Engineering Department, Los Angeles, CA 90095-1594 USA.

H. C. Lee and P. Grodzinski are with the Motorola Inc. Phoenix Corporate Research Laboratories, Tempe, AZ 85284 USA.

Publisher Item Identifier S 1041-1135(97)02414-2.

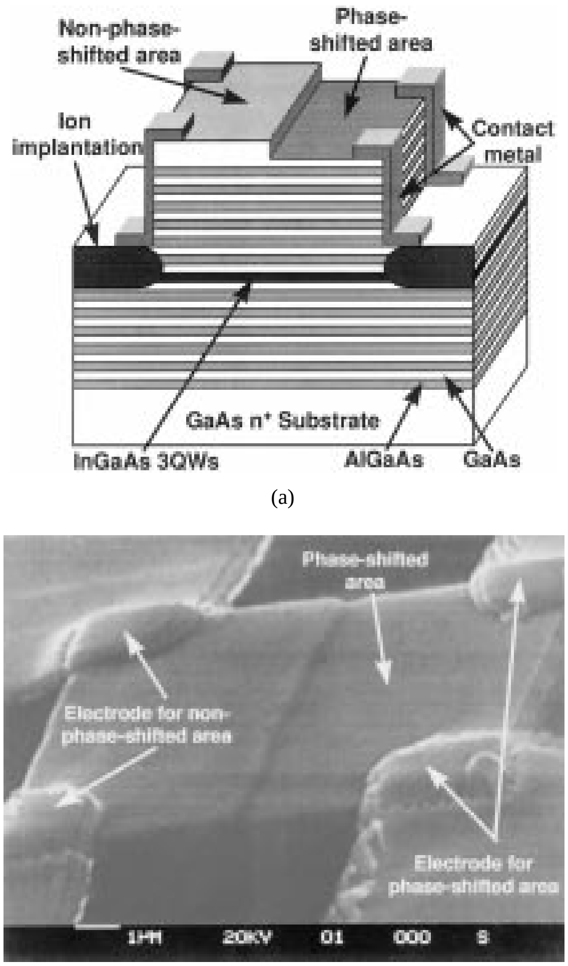

(a)

(b)

Fig. 1. (a) The schematic diagram and (b) the SEM micrograph of the VCSEL with integrated optical beam router.

is equal to half of the wavelength. The etching thickness of the optical beam router can be accurately controlled by etchstop layers or it can be achieved by depositing dielectric materials on the VCSEL surface. The switching angle can be varied by changing the spacing between the phase-shifted and nonphase-shifted regions or the refractive index of the phase-shifters.

Dynamic switching is achieved by separately pumping the phase-shifted and the nonphase-shifted regions. When both regions are pumped simultaneously, the output beam is steered away from the surface-normal direction, as described earlier. When only one region is pumped above threshold, the device becomes a normal VCSEL and the output beam switches back to the surface-normal direction. Therefore, the optical beam direction can be controlled electrically.

III. Fabrication

The fabrication processes for the beam-switched VCSEL are described in the following: The epitaxial structure is grown by metalorganic chemical vapor deposition (MOCVD). The VCSEL itself consists of a 35-pair n-doped quarter-wave GaAs–AlGaAs bottom DBR, a full-wavelength-cavity with three InGaAs–GaAs strained quantum-well active region, and a 25-pair p-doped top DBR. An extra half-wavelength-thick p^+-GaAs cap layer is grown on top of VCSEL to implement the phase-shifters. Active mesas are formed by wet chemical etching with H_2SO_4:H_2O_2:H_2O solution. The same photoresist pattern is used as a mask for a subsequent ion implantation for device isolation and lateral current confinement. After mesa etching and ion implantation, spin-on glass (SOG) is spin-coated onto the wafer at 4000 r/m for 20 s. The wafer is subsequently cured at 380 °C. The SOG is a methyl siloxane polymer solution that is often used for planarization and isolation. After curing, the SOG forms a 2000–Å-thick dielectric layer for electric isolation. Top contact windows are opened by a self-aligned process using reactive ion etching (RIE). The phase shifter, which covers half of the active mesa, is realized by etching the cap layer of the top DBR mirror. In order to maintain the fundamental mode operation, the etching depth is controlled to be half-wavelength-thick by slow wet chemical etching with H_2SO_4:H_2O_2:$H_2O = 1{:}1{:}50$ solution. The etching rate is characterized to be 1.17 nm/s. The accuracy is within $\pm 3\%$. In the future, it can be more precisely controlled by employing an etch stop layer. The VCSEL's electrodes are then deposited by metal evaporation and liftoff processes. Fig. 1(b) shows the scanning electron micrograph (SEM) of an 8 μm $\times$ 8 μm device.

IV. Experimental Results and Discussion

Dynamic switching of the optical beam router has been successfully demonstrated. Two different emitting angles are achieved by separately controlling the injection currents into the phase-shifted area and nonphase-shifted area. The far-field pattern is observed by projecting the images onto a charge-coupled device (CCD) camera. The tested device has a mesa size of 8 μm $\times$ 8 μm (both phase-shifted and nonphase-shifted areas are 4 μm $\times$ 8 μm). When only the nonphase-shifted area is pumped, most of the injection current goes to the nonphase-shifted area. The laser lases only in the nonphase-shifted area. This device behaves like a standard VCSEL and the beam emits in the surface-normal direction. The threshold current is measured to be 4.6 mA, and a circular far field pattern is observed, as shown in Fig. 2(a). When both electrodes are pumped simultaneously, the main output beam is switched to 2.9° from the surface-normal direction [Fig. 2(b)]. The total threshold current for both areas is measured to be 6.4 mA. The peak intensity of the steered beam is 10% higher than the surface-normal beam because of higher injection current. By switching on and off of the phase-shifted area, the emitting beam direction is switched back and forth between 0° and 2.9° steering angles. The full-width-at-half-maximum (FWHM) angles are 4.1° and 2.1° for the surface-normal beam and the steered beam, respectively. The surface-normal beam has broader divergence angle because it has a smaller emitting area. It is possible to make the divergence angles more symmetric by adding another separately-pumped nonphase-shifted region adjacent to the original one and pumping it only during surface-normal beam operation. The minor lob of the far field pattern in Fig. 2(b) results from the discrete-step design of the phase-shifter.

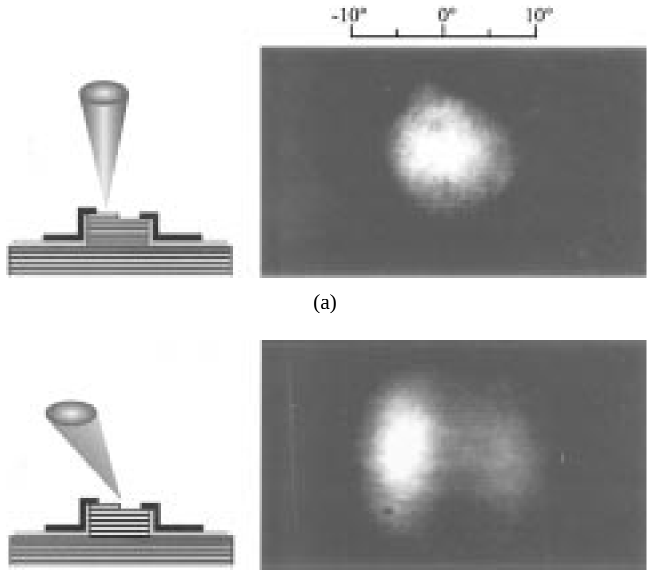

(a)

(b)

Fig. 2. Far-field patterns of the beam-switching VCSEL when current is injecting to (a) only the nonphase-shifted area; (b) both areas.

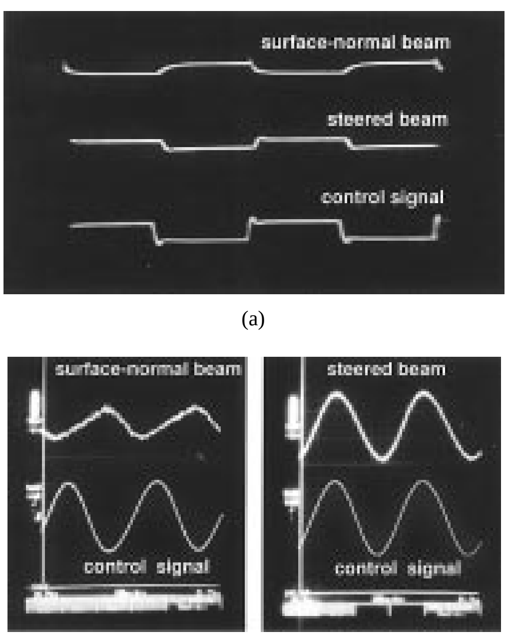

(a)

(b)

Fig. 3. Dynamic beam switching of the VCSEL when the phase-shifted area is modulated by a control signal at (a) 1 MHz and (b) 2 GHz. The surface-normal beam and the steered beam are separated by a spatial filter.

The switching speed of this device is also investigated. For this experiment, the nonphase-shifted area is biased at a fixed 5.5 mA dc current, while the phase-shifted area is connected to a control signal. An additional 1.8-mA injection current is pumped into the VCSEL phase-shifted area. These two beams are separated by a spatial filter before detected by a high-speed photodetector and displayed on an oscilloscope. Fig. 3(a) shows the dynamic switching results at 1 MHz using a square wave from a function generator as the switching source. The bottom trace displays the control signal. The top trace is the signal from surface-normal beam. It is out of phase with the control signal. The middle trace corresponds to the steered beam, which is in-phase with the control signal. Clear switching is observed. At higher frequencies, a sinusoidal wave from a frequency synthesizer is used as the control signal. For frequencies from 1 MHz to 2 GHz, clear in-phase and out-of-phase signals are observed. The switching signals at 2 GHz is shown in Fig. 3(b). The switching speed is determined by several factors. It is affected by carrier diffusion and the relaxation oscillation frequency of the VCSEL. The switching speed can be theoretically simulated by solving coupled rate equations, taking into consideration the carrier diffusion between the phase-shifted and nonphase-shifted regions. The detailed results will be presented in a later publication. By combining the beam-steering VCSEL's in two dimensions, various optical interconnect and switching networks can be realized. The beam-switching VCSEL's are very attractive for ultra compact and dense optical interconnect network for parallel computer systems.

V. Conclusion

The dynamic beam-switching in VCSEL's has been experimentally demonstrated for the first time. Optical beam switching between 0° and 2.9° from the surface-normal direction has been achieved with 8 μm $\times$ 8 μm beam-steering VCSEL's. Switching speed up to 2 GHz has been measured. This novel device maintains the advantages of VCSELs: low threshold currents (6.4 mA) and low beam divergence angles (2.1°). They are very attractive for ultra-dense optical interconnect for massively parallel computers.

References

[1] K. Hwang, *Advanced Computer Architecture: Parallelism, Scalability, Programmability*. New York: McGraw-Hill, 1993.

[2] J. W. Goodman, F. J. Leonberger, S. Y. Kung, and R. A. Athale, "Optical interconnections for VLSI systems," *Proc. IEEE*, vol. 72, pp. 850–866, July 1984.

[3] L. A. Bergman, W. H. Wu, A. R. Johnston, R. Nixon, S. C. Esener, C. C. Guest, P. Yu, T. J. Drabik, M. Feldman, and S. H. Lee, "Holographic optical interconnects for VLSI," *Opt. Eng.*, vol. 25, no. 10, pp. 1109–1118, 1986.

[4] H. S. Hinton, "Progress in systems based on free-space interconnection," in *Proc. SPIE*, vol. 1849, 1993, pp. 2–3.

[5] K. Iga, "Surface emitting lasers," *Opt. Quantum Electron.*, vol. 24, pp. S97–S104, 1992.

[6] D. L. Huffaker, J. Shin, and D. G. Deppe, "Low threshold half-wave vertical-cavity lasers," *Electron. Lett.*, vol. 30, no. 23, pp. 1946–1947, 1994.

[7] K. L. Lear, K. D. Choquette, R. P. Schneider, S. P. Kilcoyne, "Selectively oxidised vertical cavity surface emitting lasers with 50% power conversion efficiency," *Electron. Lett.*, vol. 31, no. 3, pp. 208–209, 1995.

[8] A. W. Lohmann, and D. P. Paris, "Binary Fraunhofer holograms, generated by computer," *Appl. Opt.*, vol. 6, no. 10, pp. 1739–1748, 1967.

[9] Y. Sun, C. G. Fanning, S. A. Biellak, and A. E. Siegman, "Thermal controlled lateral beam shift and beam steering in semiconductor lasers," *IEEE Photon. Technol. Lett.*, vol. 7, pp. 26–28, Jan. 1995.

[10] J. P. Hohimer, D. C. Craft, G. A. Vawter, and D. R. Myers, "Near-diffraction-limited angle-switchable output beam from a broad-area diode laser with an intracavity spatial phase controller," *Appl. Phys. Lett.*, vol. 58, no. 25, pp. 2886–2888, 1991.

[11] L. Fan, M. C. Wu, H. C. Lee, and P. Grodzinski, "Novel vertical-cavity surface-emitting lasers with integrated optical beam router," *Electron. Lett.*, vol. 31, no. 9, pp. 729–730, 1995.